

## Background study of NaI(Tl) crystals for the KIMS-NaI experiment

This content has been downloaded from IOPscience. Please scroll down to see the full text.

2016 J. Phys.: Conf. Ser. 718 042001

(<http://iopscience.iop.org/1742-6596/718/4/042001>)

View [the table of contents for this issue](#), or go to the [journal homepage](#) for more

### Download details:

IP Address: 203.255.172.21

This content was downloaded on 01/11/2016 at 06:23

Please note that [terms and conditions apply](#).

You may also be interested in:

[WIMPs search by means of thin NaI\(Tl\) array](#)

K Fushimi, H Kawasuso, E Aihara et al.

[Analytic Calculation of Photofractions for NaI\(Tl\) Scintillation Crystals to Monoenergetic Gamma Rays](#)

Kunio Kaminishi

[Dark matter searches with NaI scintillators in the Canfranc underground laboratory: ANAIS experiment](#)

J Amaré, B Beltrán, J M Carmona et al.

[Experimental validation of response function of a NaI \(Tl\) detector modeled with Monte Carlo codes](#)

M.T. Hajheidari, M.J. Safari, H. Afarideh et al.

[Cosmic-Ray Contribution to the Background of NaI Scintillation Spectrometers](#)

Eiichi Tanaka, Susumu Itoh, Toshiyuki Hiramoto et al.

[Field Emission Studies of Sodium Iodide and Mercury on Tungsten](#)

Hiroshi Washimi

# Background study of NaI(Tl) crystals for the KIMS-NaI experiment

P Adhikari<sup>1</sup>, G Adhikari<sup>1</sup>, S Choi<sup>2</sup>, C Ha<sup>3</sup>, I S Hahn<sup>4</sup>, EJ Jeon<sup>3</sup>, H W Joo<sup>2</sup>, W G Kang<sup>3</sup>, H J Kim<sup>5</sup>, H O Kim<sup>3</sup>, K W Kim<sup>2</sup>, N Y Kim<sup>3</sup>, S K Kim<sup>2</sup>, Y D Kim<sup>1,3</sup>, Y H Kim<sup>3,6</sup>, H S Lee<sup>3</sup>, J H Lee<sup>3</sup>, M H Lee<sup>3</sup>, D S Leonard<sup>3</sup>, J Li<sup>3</sup>, S Y Oh<sup>1</sup>, S L Olsen<sup>3</sup>, H K Park<sup>3</sup>, H S Park<sup>6</sup>, K S Park<sup>3</sup>, J H So<sup>3</sup>, Y S Yoon<sup>3</sup>

<sup>1</sup> Department of Physics, Sejong University, Seoul 05006, Korea

<sup>2</sup> Department of Physics and Astronomy, Seoul National University, Seoul 08826, Korea

<sup>3</sup> Center for Underground Physics, Institute for Basic Science, Daejeon 34047, Korea

<sup>4</sup> Department of Science Education, Ewha Womans University, Seoul 03760, Korea

<sup>5</sup> Department of Physics, Kyungpook National University, Daegu 41566, Korea

<sup>6</sup> Korea Research Institute of Standards and Science, Daejeon 34113, Korea

**Abstract.** The DAMA experiment has reported an annual-modulation signal in an array of low-background NaI(Tl) scintillating crystals that may be caused by WIMP-nucleon interactions. However, to date there has been no direct confirmation of this result that uses the same target nuclides. The Korea Invisible Mass Search (KIMS) collaboration has been engaged in an extensive R&D program to grow ultra-low background NaI(Tl) crystals for use as a direct test of the DAMA result using same nuclide targets. Six crystals were grown from different powders in order to understand mechanisms of internal background contaminations and to reduce their effects. Studies of internal backgrounds in these crystals were performed with the ultimate goal of reducing internal background contamination levels to 1 dnu at 2 keV.

## 1. Introduction

The Korea Invisible Mass Search (KIMS) experiment searched for weakly interacting massive particles (WIMP) dark matter using an array of ultra-low-background CsI(Tl) crystal detectors at the Yangyang Underground laboratory (Y2L) near the east coast of the Korean peninsula [1, 2]. The DAMA/LIBRA experiment has claimed the observation of an annual modulation signature similar to that which would be produced by WIMPs [3] while other experiments, including KIMS-CsI [4, 5], reported null results. However, alternative interpretations of the DAMA/LIBRA results as being primarily due to WIMP-sodium nuclei interactions, which would be the case for low-mass WIMPs, cannot be ruled out. Therefore, it is necessary to try to reproduce the DAMA/LIBRA observations with crystal detectors of the same NaI(Tl) composition.

## 2. The Experimental Setup

We used the Y2L experimental setup that was used for the KIMS-CsI experiment [5, 6] to measure background contamination levels in various NaI(Tl) crystals. This includes a 12-module array of CsI(Tl) crystals inside a shield that consists, from inside out, of 10 cm of copper, 5 cm



of polyethylene, 15 cm of lead, and 30 cm of liquid-scintillator-loaded mineral oil. This shielding attenuates external neutrons and gamma rays, and vetoes cosmic-ray muons. Six R&D-stage NaI(Tl) crystals were tested inside the CsI(Tl) detector array using a configurations as shown in Fig. 1.

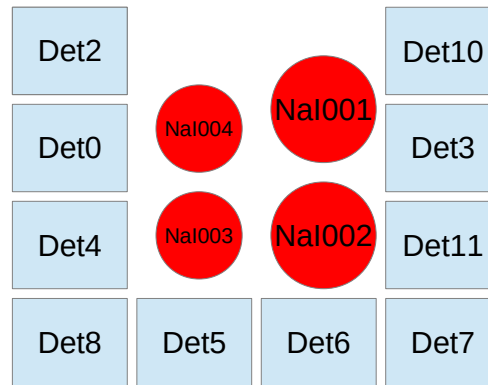


**Figure 1.** Schematic view of the NaI(Tl) (circles) and CsI(Tl) (squares) crystal arrangements used for the measurements reported here. In the later tests, NaI-003 and NaI-004 were replaced by NaI-005 and NaI-006.

**Table 1.** Specifications of the NaI(Tl) crystals. The “Powder” acronyms are AS-B (AS-C): Alpha Spectra purified powder, SA-AG: Sigma-Aldrich Astro-Grade powder (reduced K content), SA-CG: Sigma-Aldrich Crystal-Growth powder, and AS-WSII: Alpha Spectra WIMPScint-II grade powder. The names of the crystal growing companies are abbreviated as AS: Alpha-Spectra and BH: Beijing-Hamamatsu. The last two columns are the months the crystals were grown and transported to Y2L.

Crystal	Size (D×L)	Powder	Company	T (Growth)	T (Y2L)
NaI-001	5'' × 7''	AS-B	AS	2011.9	2013.9
NaI-002	4.2'' × 11''	AS-C	AS	2013.4	2014.1
NaI-003	4.5'' × 3.5''	SA-AG	AS	2014.4	2014.9
NaI-004	4.5'' × 3.5''	SA-CG	AS	2014.3	2014.9
NaI-005	4.2'' × 11''	AS-WSII	AS	2014.7	2014.12
NaI-006	4.8'' × 8.8''	SA-CG	BH	2014.10	2015.1

### 3. Internal Natural Backgrounds

The production of ultralow background crystals requires a comprehensive understanding of the internal contamination of natural radioisotopes in existing crystals. Table 2 lists the contamination levels for the six crystals as measured with the test configurations described above.

*3.0.1. <sup>40</sup>K background* In our setup, <sup>40</sup>K decays are identified by coincidence signals between 1460 keV  $\gamma$ -rays in the CsI(Tl) detectors and 3 keV X-rays in the NaI(Tl). Fig. 2 (left) shows

**Table 2.** Background rates from internal radioactive contaminants in the NaI(Tl) crystals. Chain equilibrium was assumed for the interpretation of radioactivity measurements related to  $^{238}\text{U}$  and  $^{232}\text{Th}$ . For the “ $\alpha$  Rate”, each alpha particle is counted as one decay.

Crystal (unit)	$^{\text{nat}}\text{K}$ ( $^{40}\text{K}$ ) (ppb)	$^{238}\text{U}$ (ppt)	$^{232}\text{Th}$ (ppt)	$\alpha$ Rate (mBq/kg)	Light Yield (Photoelectrons/keV)
NaI-001	$40.4 \pm 2.9$	$< 0.02$	$< 3.2$	$3.29 \pm 0.01$	$15.6 \pm 1.4$
NaI-002	$48.1 \pm 2.3$	$< 0.12$	$0.5 \pm 0.3$	$1.77 \pm 0.01$	$15.5 \pm 1.4$
NaI-003	$25.3 \pm 3.6$	$< 0.14$	$0.5 \pm 0.1$	$2.43 \pm 0.01$	$13.3 \pm 1.3$
NaI-004	$> 116.7$	—	—	—	$3.9 \pm 0.4$
NaI-005	$40.1 \pm 4.2$	$< 0.04$	$0.2 \pm 0.1$	$0.48 \pm 0.01$	$12.1 \pm 1.1$
NaI-006	$> 127.1$	$< 0.05$	$8.9 \pm 0.1$	$1.53 \pm 0.01$	$4.4 \pm 0.4$

a scatter plot of NaI vs CsI energies for coincidence events; the  $^{40}\text{K}$  signal is the small island of  $\sim 3$  keV NaI(Tl) signals and  $\sim 1460$  keV CsI signals. Fig. 2 (right) shows the energy spectrum of events in the NaI crystal that are in coincidence with an  $E = 1460 \pm 150$  KeV signal in one of the CsI counters. The  $^{40}\text{K}$  background level in each crystal is determined by comparing the measured coincidence rate with a Geant4-simulated rate using the method described in Ref. [6].

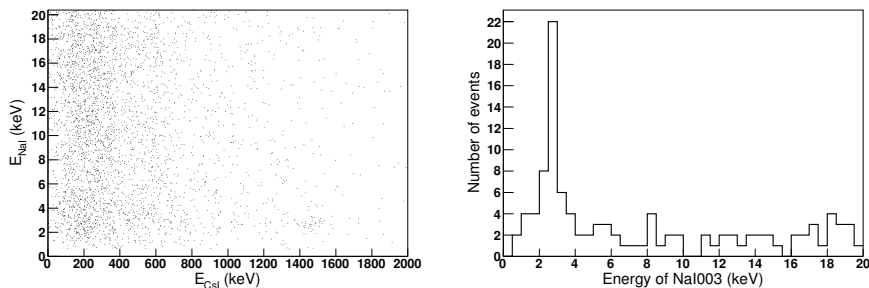


**Figure 2.** (left) A scatterplot of NaI-003 signals (vertical) versus CsL crystal energies (horizontal) for coincidence events. (right) The NaI-003 crystal’s energy distribution for events in coincidence with a  $1460 \pm 150$  keV  $\gamma$ -ray in one of the CsI crystals. The  $^{40}\text{K}$  events correspond to the distinct peak near 3 keV in the NaI-003 detector’s energy spectrum.

From these data we determine that NaI-003 crystal, which was grown from SA-AG powder, has a  $^{\text{nat}}\text{K}$  contamination level of  $25.3 \pm 3.6$  ppb. This is the lowest  $^{\text{nat}}\text{K}$  contamination of all of the six tested crystals and is in good agreement with the vendor’s ICP-MS measurement of 25 ppb for this powder. Due to low light yields from NaI-004 and NaI-006, which were made with SA-CG powder, we are only able to establish lower limits on the  $^{\text{nat}}\text{K}$  contamination levels of more than 100 ppb, consistent with the listed contamination levels for the SA-CG powder.

Based on these measurements, we conclude that the source of  $^{40}\text{K}$  contamination in the NaI(Tl) crystals is mostly from contamination in the NaI powder, and no significant amount of contamination is introduced during the crystal growing procedure. The  $^{\text{nat}}\text{K}$  measurements for the six crystals are listed in Table 2.

The  $^{\text{nat}}\text{K}$  content in the DAMA crystals are in the 10–20 ppb range [11]. Further R&D on procedures for additional potassium reduction in the NaI powder are in progress. In the near future, the potassium background is expected to be reduced to a level lower than the level which was achieved by DAMA/LIBRA.

*3.0.2.  $^{238}\text{U}$  background* Assuming equilibrium in the  $^{238}\text{U}$  decay chain, we can evaluate the contamination level in the NaI(Tl) crystals by exploiting the  $237\ \mu\text{s}$  mean lifetime of  $^{214}\text{Po}$   $\alpha$ -decay, which immediately follows its production via  $\beta$ -decay of  $^{214}\text{Bi}$  as described in Refs. [6]. Using pulse shape differences to distinguish between  $\alpha$ -induced and  $\beta$ -induced events, we can determine  $^{238}\text{U}$  contamination levels in the six crystals. We found no significant time-dependent exponential components that are a characteristic of  $^{214}\text{Po}$  and from this we infer that the  $^{238}\text{U}$  background levels in the crystals are all below the ppt level (see Table 2).

*3.0.3.  $^{232}\text{Th}$  background* Contamination from the  $^{232}\text{Th}$  decay chain was studied by using  $\alpha - \alpha$  time interval measurements in the crystals. In this case, we looked for a  $^{216}\text{Po}$   $\alpha$ -decay component that has a mean decay time of 209 ms that follows its production via the  $\alpha$ -decay of  $^{220}\text{Rn}$ . Figure 3 (right) shows distributions of the time differences between two adjacent  $\alpha$ -induced events in NaI-006, which shows a clear  $^{216}\text{Po}$  signal. The  $^{232}\text{Th}$  contents in all of the crystals, inferred assuming chain equilibrium, are listed in Table 2.

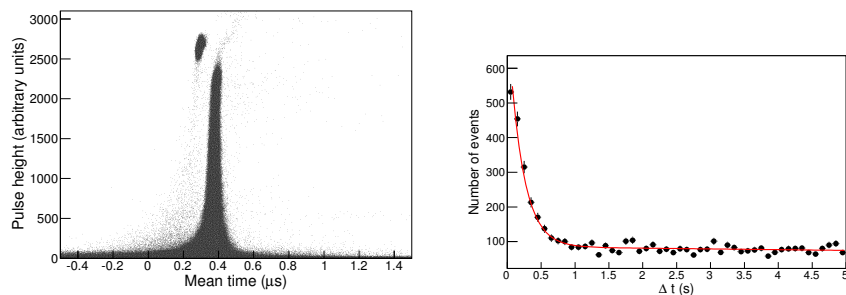


**Figure 3.** (left) A scatter plot of Mean time (horizontal) versus pulse height (vertical). The distinct island of events with high energies and smaller mean times are due to  $\alpha$ -induced events. (right) The time difference distribution between two successive  $\alpha$ -induced events in the NaI-006 crystal.

*3.0.4.  $^{210}\text{Pb}$  background* In the  $^{222}\text{Rn}$  decay chain,  $^{210}\text{Po}$  (half life = 138 days), produced by the beta decay of  $^{210}\text{Pb}$  (half life = 22 years) and  $^{210}\text{Bi}$  (half life = 5 days), subsequently decays via alpha emission to  $^{206}\text{Pb}$ . Thus, at the time that an  $^{222}\text{Rn}$  contamination occurs, if the  $^{210}\text{Po}$  contamination is zero, it will grow with a characteristic time of  $\tau_{\text{Po}} = 200$  days until an equilibrium is reached. This change in the total alpha rate over time can be used to infer the date that the  $^{222}\text{Rn}$  contamination occurred. Figure 4(left) shows the total alpha rates in a crystal as a function of data-taking time (in days).

The  $^{210}\text{Po}$  alpha activity grows as

$$R_{\alpha}(t) \approx A(1 - e^{-(t-t_0)/\tau_{\text{Po}}}), \quad (1)$$

where  $t_0$  is the time when the initial  $^{210}\text{Pb}$  contamination occurred, assuming that the contamination occurred over a single short time period. The fits to the time dependence of the  $^{210}\text{Po}$  alpha signals shown in Fig. 4 (left) indicate that  $t_0$  occurs around the time that the crystal was grown. However, since the preparation of the NaI powder takes place about two months prior to the crystal growing, it is still possible that some contamination occurred during the powder production procedures.

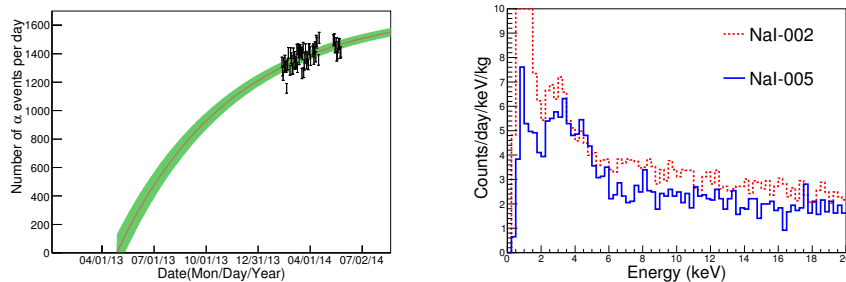


**Figure 4.** (left) The measured increases in alpha activity is fitted to a model that assumes a single, instantaneous  $^{210}\text{Po}$  contamination event occurred for each crystal. (right) Background event spectra for energies below 20 keV in the NaI-002 (red line) and NaI-005 (blue line) crystals.

*3.0.5. Background summary* Figure 4 (right) shows a comparison of background levels in the NaI-002 and NaI-005 crystals. The factor of three reduction of  $^{210}\text{Pb}$  that is observed in NaI-005 compared to that for NaI-002 encourages us to expect to be able to achieve a 2 dru (differential rate unit = counts/day/keV/kg) background level at 6 keV. Below 6 keV,  $^{40}\text{K}$  X-rays and cosmogenic activations of I, Te, and  $^{22}\text{Na}$  isotopes are the main contributors to the remaining background. These cosmogenically activated backgrounds are expected to disappear after a year deep underground at Y2L [14].

To understand background contributions from internal radioisotopes, we used Geant4-based Monte-Carlo simulations. From these we determine that a 40 ppb contamination of  $^{\text{nat}}\text{K}$  in NaI-005 produces a background count rate of approximately 0.7 dru in the 2–4 keV energy range. This will be further reduced in crystals grown from a different batch of an SA-AG powder (10 ppb) or by using an AS-WSIII powder (16 ppb) for future crystals. The submersion of the crystal array in a surrounding liquid scintillating veto system (LSV) will further reduce backgrounds from  $^{40}\text{K}$  events and bring this background contribution to below the 0.2 dru level.

For the  $^{210}\text{Pb}$  contaminations in the crystals, the contribution to the total background in NaI-005 is already at about the 0.5 dru level for energies below 10 keV. The development of chemical purification techniques using ion-exchange resins to remove  $^{210}\text{Pb}$  from the NaI powder would lead to an additional reduction of the  $^{210}\text{Pb}$  background by a factor of two (to less than 0.3 dru).

#### 4. Conclusion

We procured and tested six NaI(Tl) crystals as part of a program to develop ultra-low-background NaI(Tl) crystals for WIMP searches. We have reduced the  $^{210}\text{Pb}$  and  $^{40}\text{K}$  backgrounds in some crystals and have achieved a 2 dru background level for recoil energies around 6 keV. Additional powder purification procedures and the implementation of an LSV system should further reduce the background level to about 1 dru.

#### Acknowledgments

This research was funded by the Institute for Basic Science (Korea) under project code IBS-R016-D1 and was supported by the Basic Science Research Program through the National Research Foundation of Korea funded by the Ministry of Education (NRF-2011-35B-C00007).

#### References

- [1] Kim Y *et al* 2005 *Nucl.Instrum.Meth.A.* **552** 456
- [2] Lee H *et al* 2005 *Nucl.Instrum.Meth.A.* **571** 644

- [3] Bernabei R *et al* (DAMA/LIBRA Collaboration) 2010 *Eur. Phys. J. C* **67** 39
- [4] Lee H *et al* (KIMS Collaboration) 2007 *Phys. Rev. Lett.* **99** 091301
- [5] Kim S *et al* (KIMS Collaboration) 2012 *Phys. Rev. Lett.* **108** 181301
- [6] Kim K *et al* 2015 *Astropart. Phys.* **62** 249
- [7] Aoruke E *et al* (XENON100 Collaboration) 2012 *Phys. Rev. Lett.* **109** 181301
- [8] Akerib D *et al* (LUX Collaboration) 2014 *Phys. Rev. Lett.* **112** 091303
- [9] Agness R *et al* (CDMS Collaboration) 2014 *Phys. Rev. Lett.* **112** 041302
- [10] Lee H *et al* (KIMS Collaboration) 2006 *Phys. Lett. B* **633** 201
- [11] Bernabei R *et al* 2008 *Nucl. Instrum. Methods Phys. Res., Sect. A* **592** 3
- [12] Gerbier G *et al* 1999 *Astropart. Phys.* **11** 287
- [13] Lee H *et al* 2014 *JINST* **9** P11015
- [14] Amare J *et al* 2015 *J. Cosmol. Astropart. Phys.* **1502** 046